Harnessing the power of mm-wave intensity mapping to study early galaxy formation

Guochao (Jason) Sun | CIERA Fellow at Northwestern University

Collaborators: T. Nguyen, T. Starkenburg, B. Scott, C.-A. Faucher-Giguère (NU/CIERA/SkAI)
A. Lidz (Penn), T.-C. Chang (JPL), S. Furlanetto (UCLA)

mm Universe 2025 | University of Chicago | June 27, 2025

CELEBRATING CIERA 15 YEARS

SkAI

Funded by the U.S. National Science Foundation and the Simons Foundation

High-redshift Universe: fascinating by its many unknowns

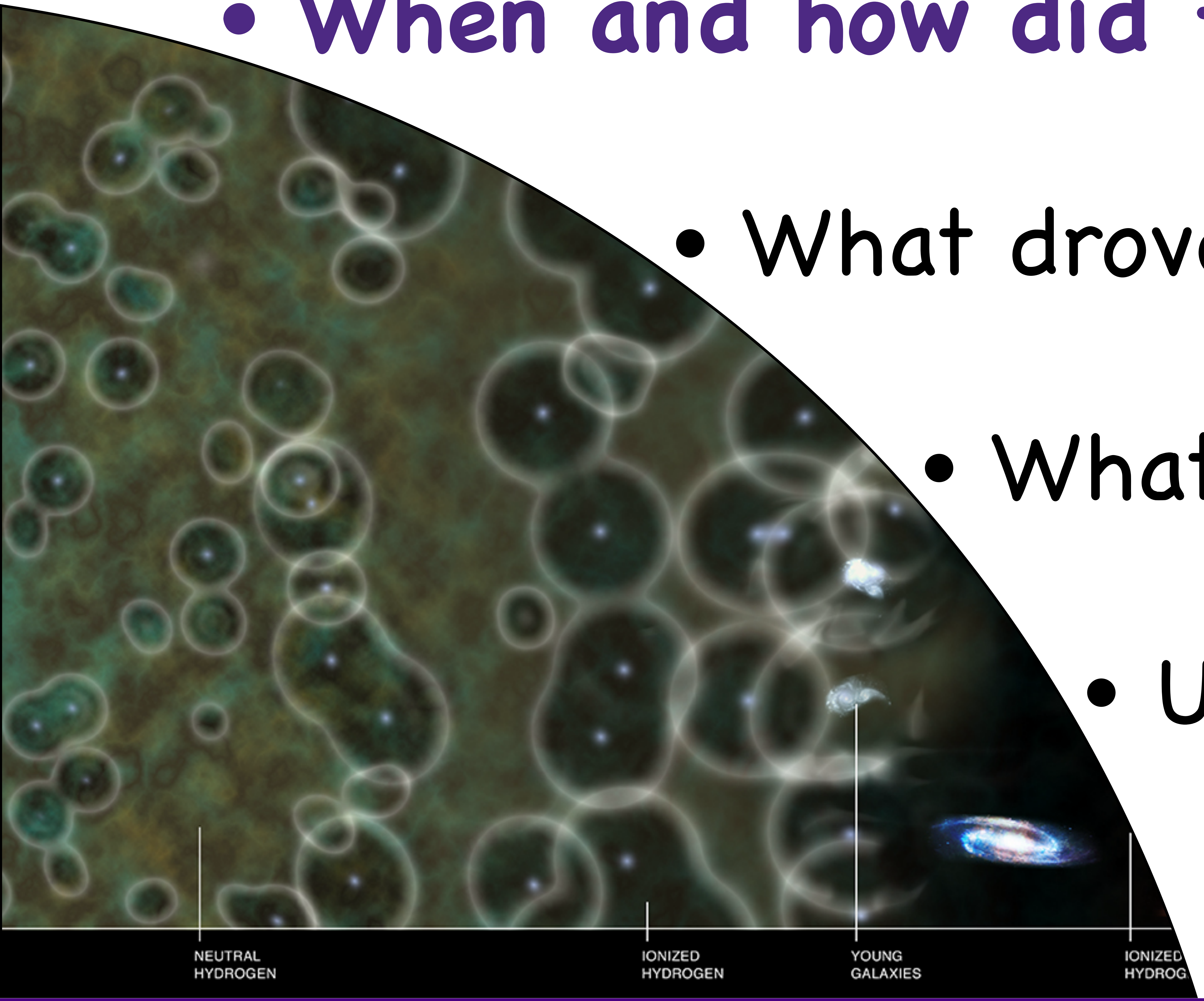

- **When and how did first galaxies form?**
- What drove cosmic reionization and how?
- What were first black holes like?
- Unique lab for new physics?

LIMFAST: 21cmFAST extension for multi-tracer IM

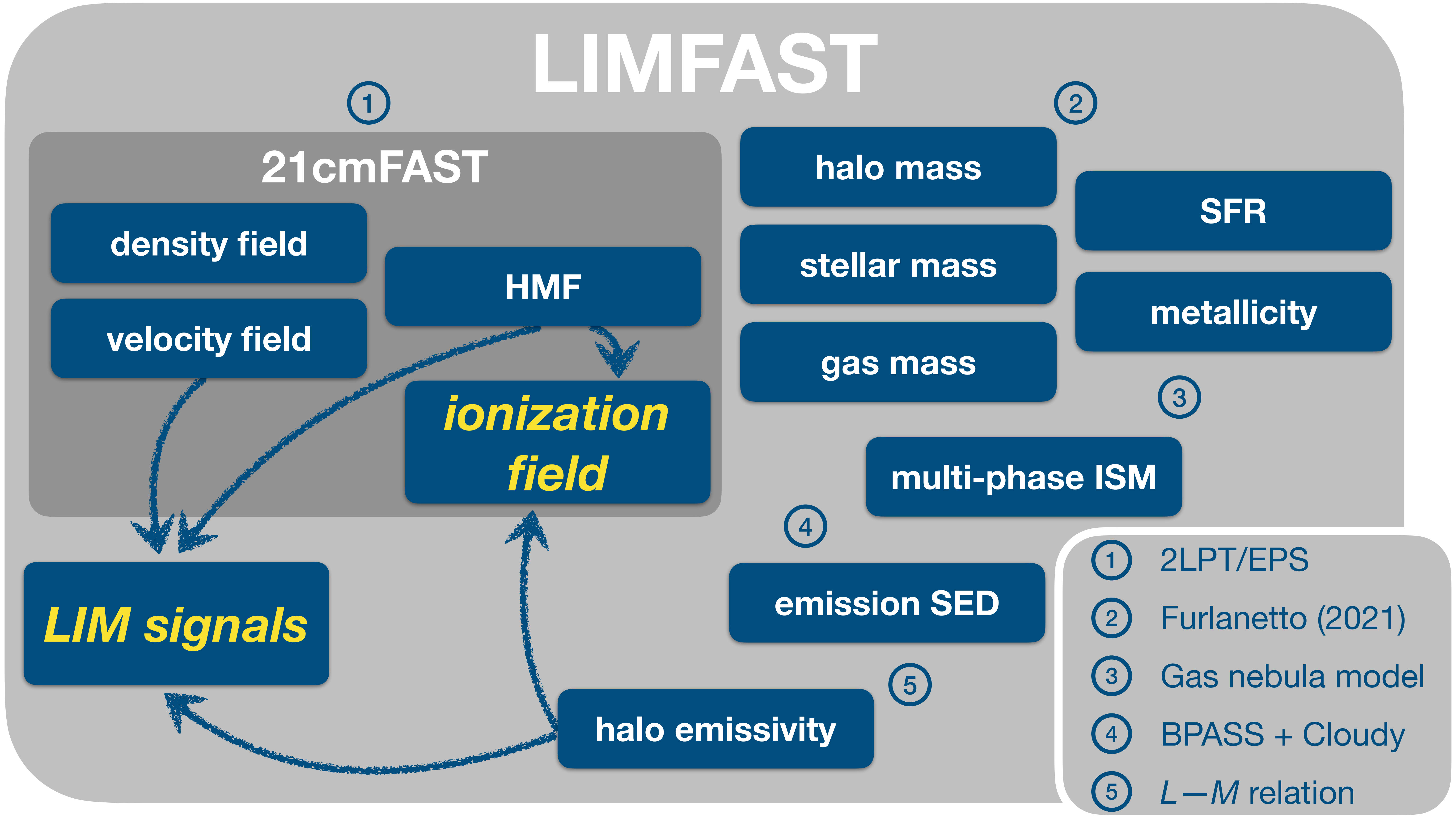

- L. Mas-Ribas, **GS** et al. (2023): Methodology & LIM predictions
- **GS** et al. (2023): LIM for high-z galaxy formation
- **GS** et al. (2025): 21cm^2—NIRB cross-correlation
- **GS et al. (2025, in prep.): Parameter inference from LIM**

Gas-regulator model for feedback-regulated star formation

Mass loading factor

$$\eta(M_\mathrm{h}, z) = \eta_0 \left(\frac{M_\mathrm{h}}{10^{11.5}\, M_\odot} \right)^{-\xi} \left(\frac{1+z}{9} \right)^{-\xi_z}$$

Star formation law

$$\dot{\Sigma}_\star(\Sigma_\mathrm{g}, z) = \epsilon_{\star,0} \frac{\Sigma_{\mathrm{g},0}}{t_{\mathrm{ff},0}^{\mathrm{disc}}} \left(\frac{\Sigma_\mathrm{g}}{\Sigma_{\mathrm{g},0}} \right)^{\zeta} \left(\frac{1+z}{9} \right)^{\zeta_z}$$

- ξ — M_h dependence of mass loading factor
- ξ_z — z dependence of mass loading factor
- ζ — slope of star formation law

Halo mass

$$\frac{\tilde{M}_\mathrm{h}'}{\tilde{M}_\mathrm{h}} = -\mathscr{M}_0$$

Gas mass

$$\frac{\tilde{M}_\mathrm{g}'}{\tilde{M}_\mathrm{g}} = \mathscr{M}_0 \left[-\frac{1}{X_\mathrm{g}} + \eta_0 \dot{X}_{\star,0} \left(\frac{X_\mathrm{g}}{X_{\mathrm{g},0}} \right)^{\alpha_X} \tilde{M}_\mathrm{h}^{\alpha_m} \left(\frac{1+z}{1+z_0} \right)^{\alpha_z} \right]$$

Stellar mass

$$\tilde{M}_\star' = -\mathscr{M}_0 \dot{X}_{\star,0} \left(\frac{X_\mathrm{g}}{X_{\mathrm{g},0}} \right)^{\beta_X} \tilde{M}_\mathrm{h}^{\beta_m} \left(\frac{1+z}{1+z_0} \right)^{\beta_z}$$

Gas retention

$$\frac{X_\mathrm{g}'}{X_\mathrm{g}} = \frac{\tilde{M}_\mathrm{g}'}{\tilde{M}_\mathrm{g}} - \frac{\tilde{M}_\mathrm{h}'}{\tilde{M}_\mathrm{h}}$$

Metal mass

$$\tilde{M}_Z' = \left[y_Z - \eta \left(\tilde{M}_Z / \tilde{M}_\mathrm{g} \right) \right] \tilde{M}_\star'$$

GS et al. (2025, in prep.; see also S. Furlanetto 21)

Halo properties respond differently to SFE & SF law

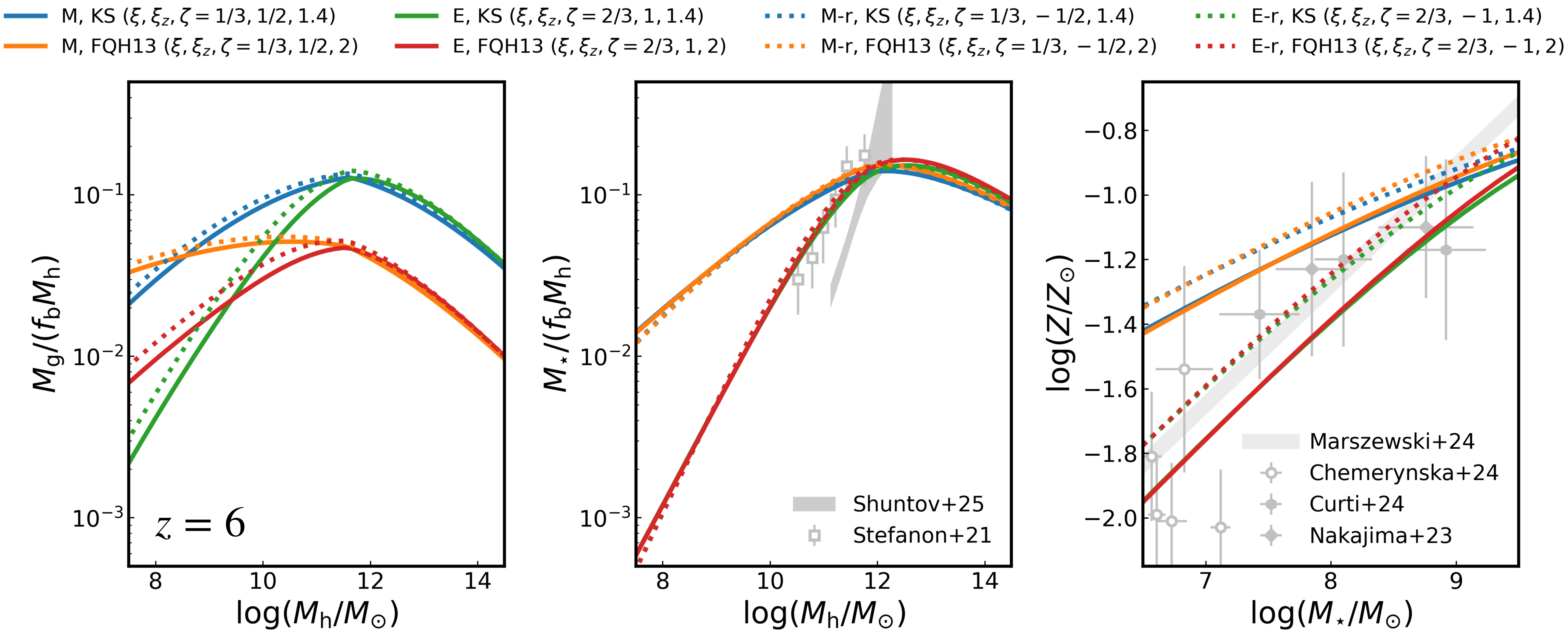

GS et al. (2025, in prep.)

Multi-line emission: a toy model of multi-phase gas nebula

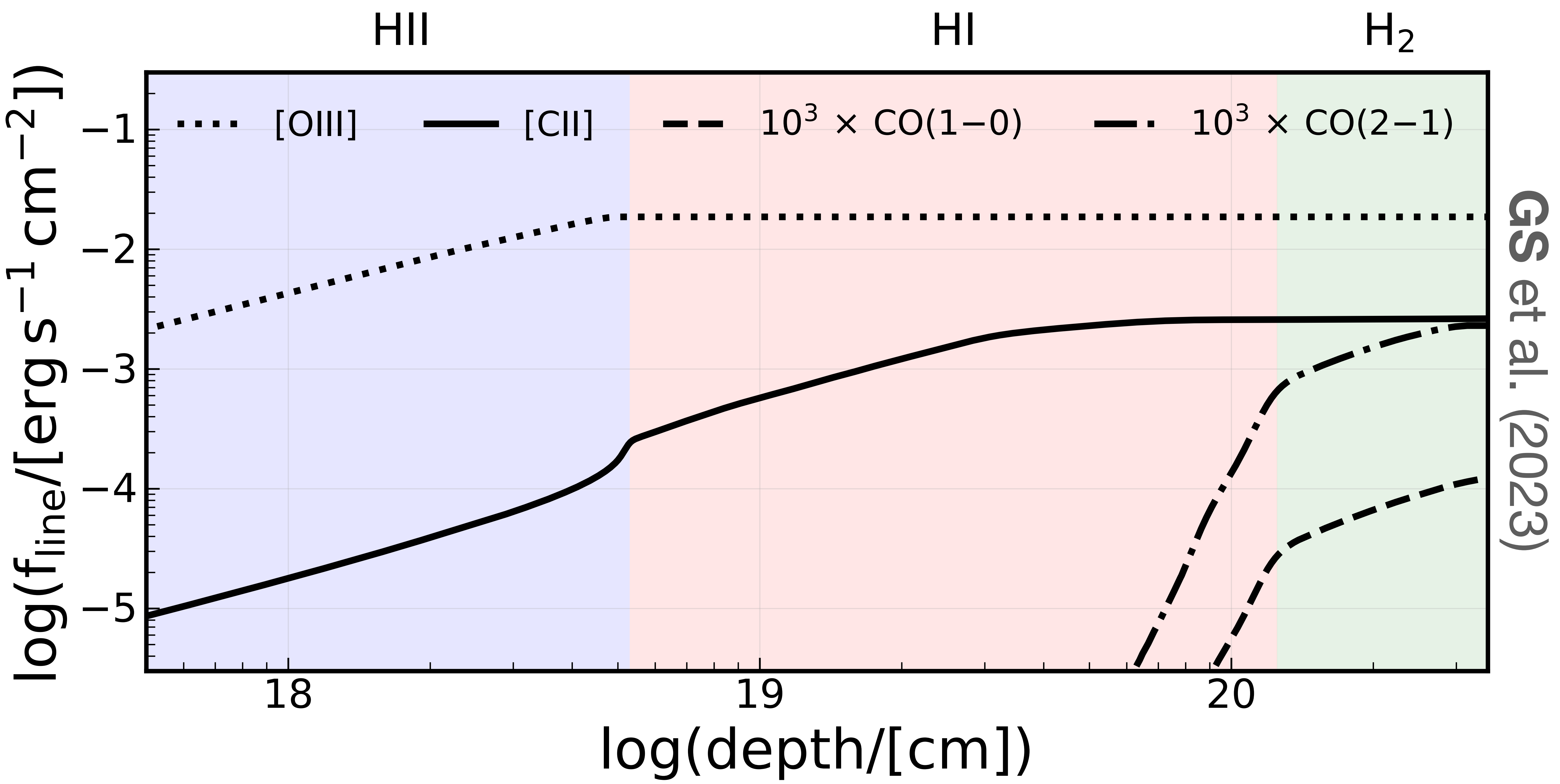

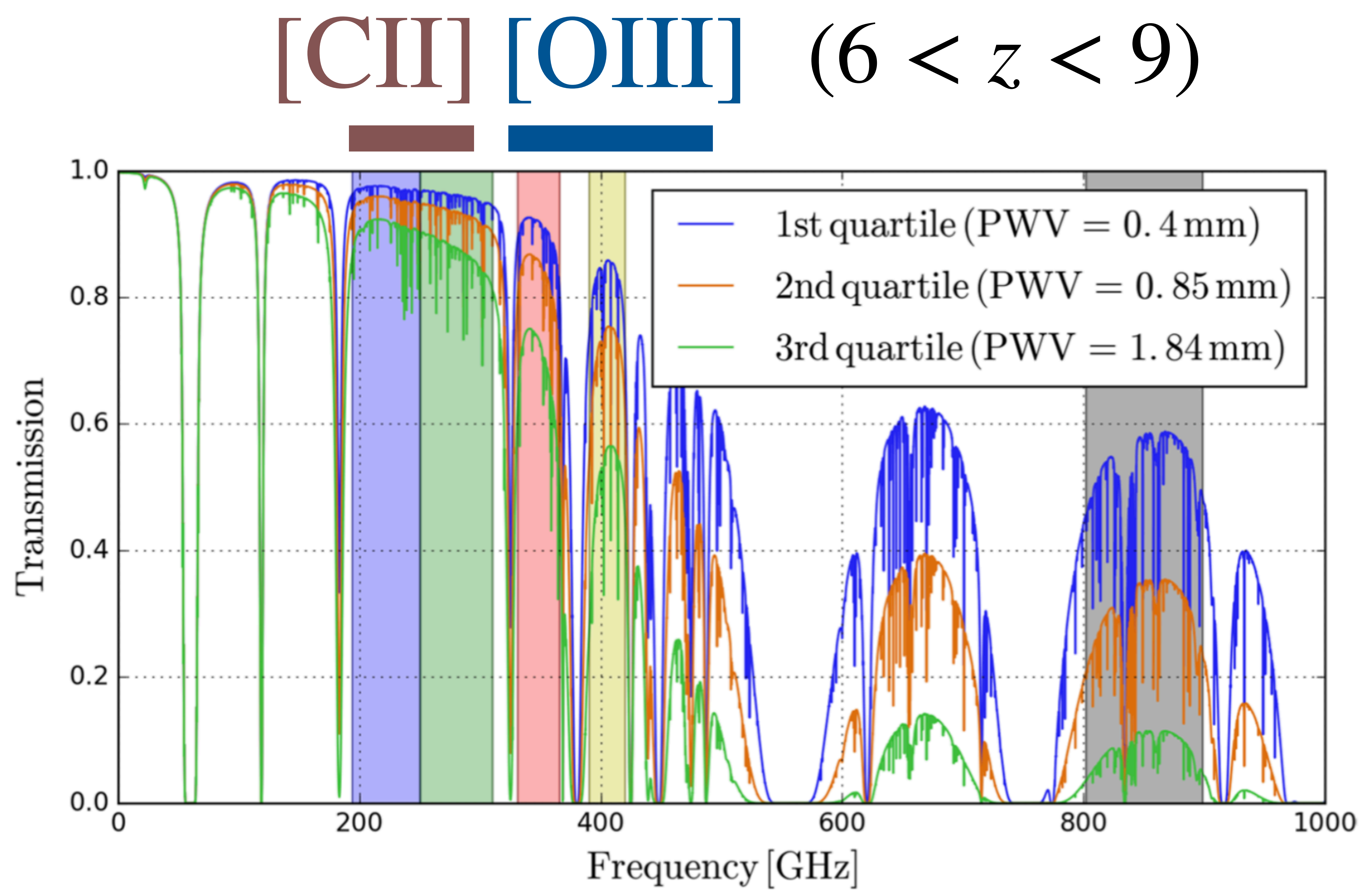

S. Choi et al. (2020)

- **CLOUDY-based line emissivities**
- **Convolved w/ turbulent GMC density PDF**
- **Scaled by halo stellar/gas mass content**

$L_{[CII]}$ & $L_{[OIII]}$ under varying SFE & SF law assumptions

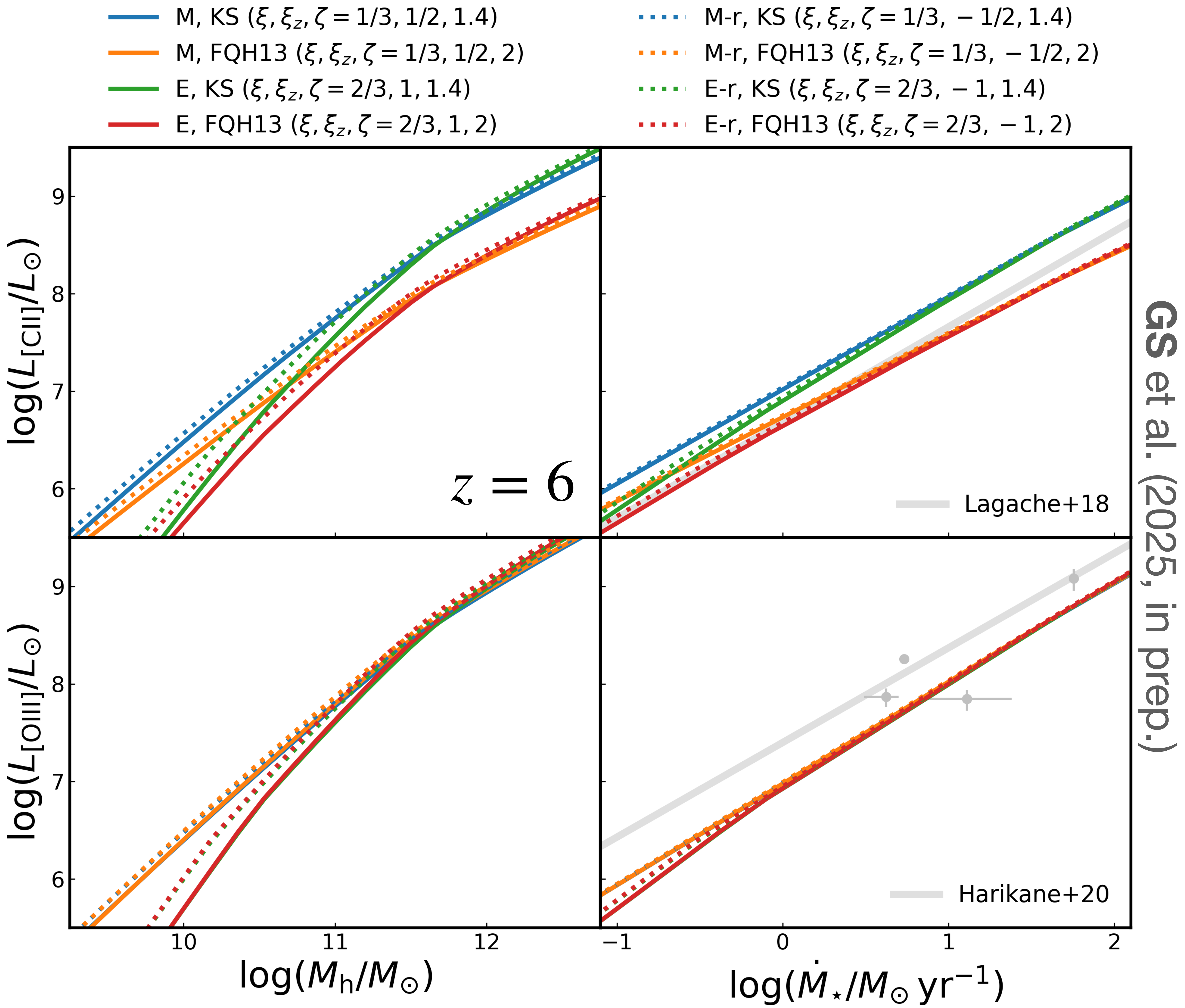

- **[CII] affected by feedback & SF law**
- **[OIII] affected solely by feedback**

Simulating [CII], [OIII], and their cross-correlation w/ LBGs

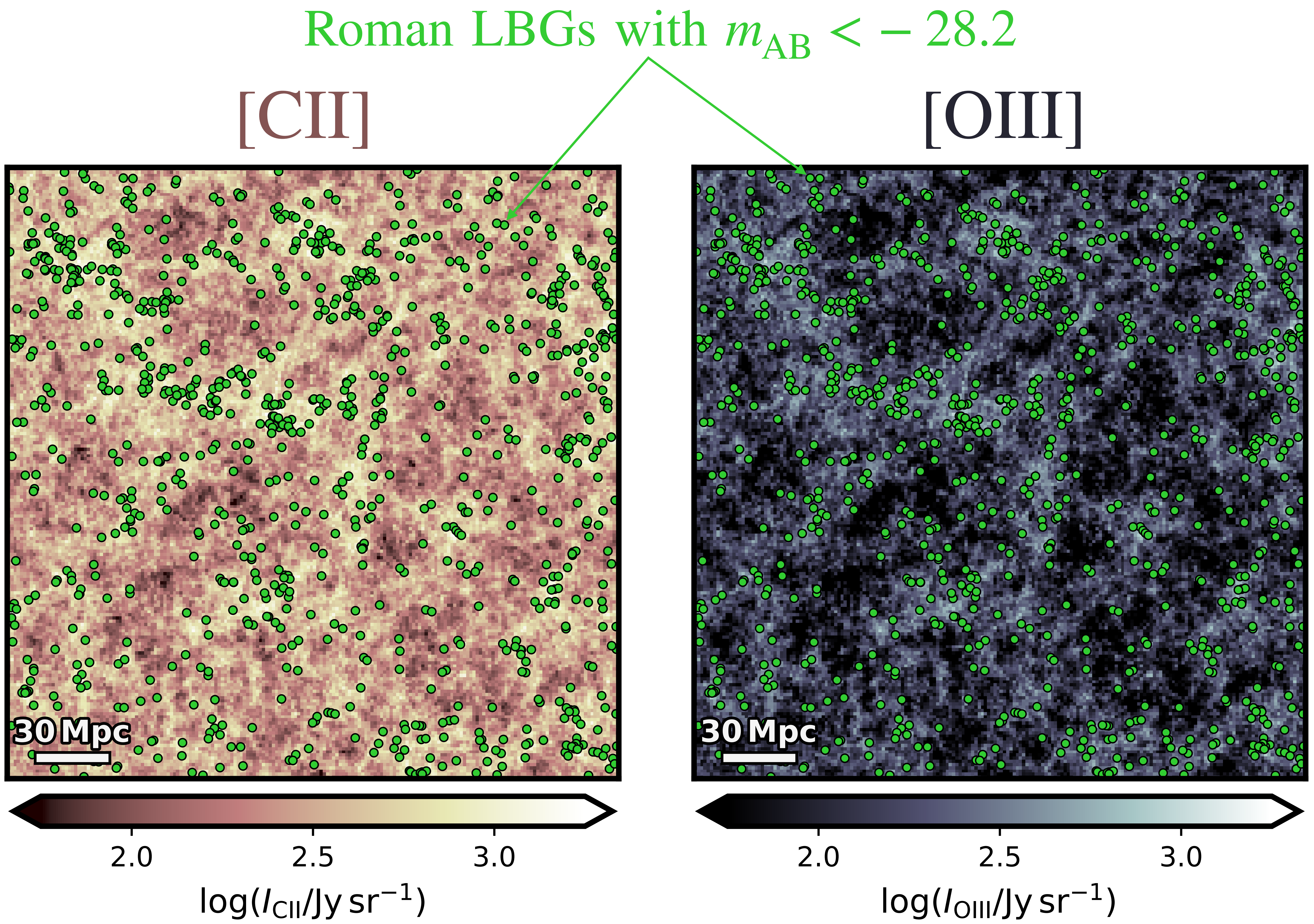

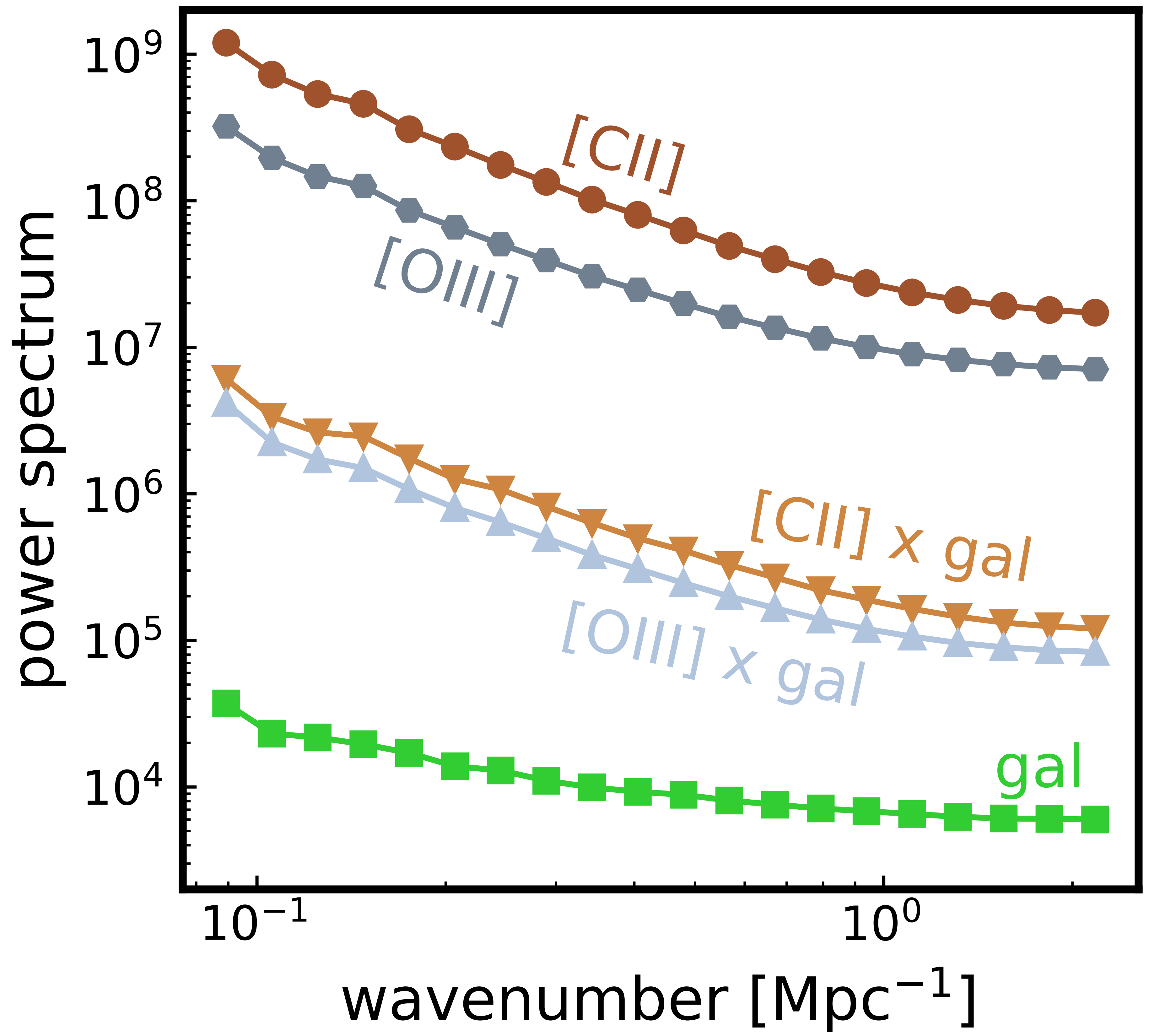

GS et al. (2025, in prep.)

Fisher matrix forecasts for [CII] & [OIII] joint analysis

Table 1. Survey and instrument specifications of the [C II] and [O III] LIM surveys considered in this work

Target	Redshifts	Bandpass (GHz)	D_{ap} (m)	Ω_{survey} (deg^2)	t_{survey} (hr)	N_{pix}	R	Ω_{beam} ($'^2$)	V_{vox} (Mpc^3)	σ_N (Jy sr^{-1} s$^{1/2}$)	P_N ((Jy sr^{-1})^2 Mpc^3)
Current-generation survey (ground-based, FYST-like)											
[C II]	6, 7, 8, 9	190–270	10	4	4000	1000	100	0.3	67	2×10^6	3×10^9
[O III]	7.5, 8.5	360, 400	10	4	4000	1000	100	0.1	23	4×10^6	1.2×10^{10}
Next-generation survey (space-based, P22-like)											
[C II]	6, 7, 8, 9	190–270	3	4	1000	100	100	3	750	2×10^5	1.2×10^9
[O III]	6, 7, 8, 9	340–490	3	4	1000	100	100	1	230	2×10^5	1.2×10^9

NOTE—Reference values of Ω_{beam}, V_{vox}, and P_N are given at $z = 7$ (7.5 for ground-based [O III]).

Current, CCAT-like

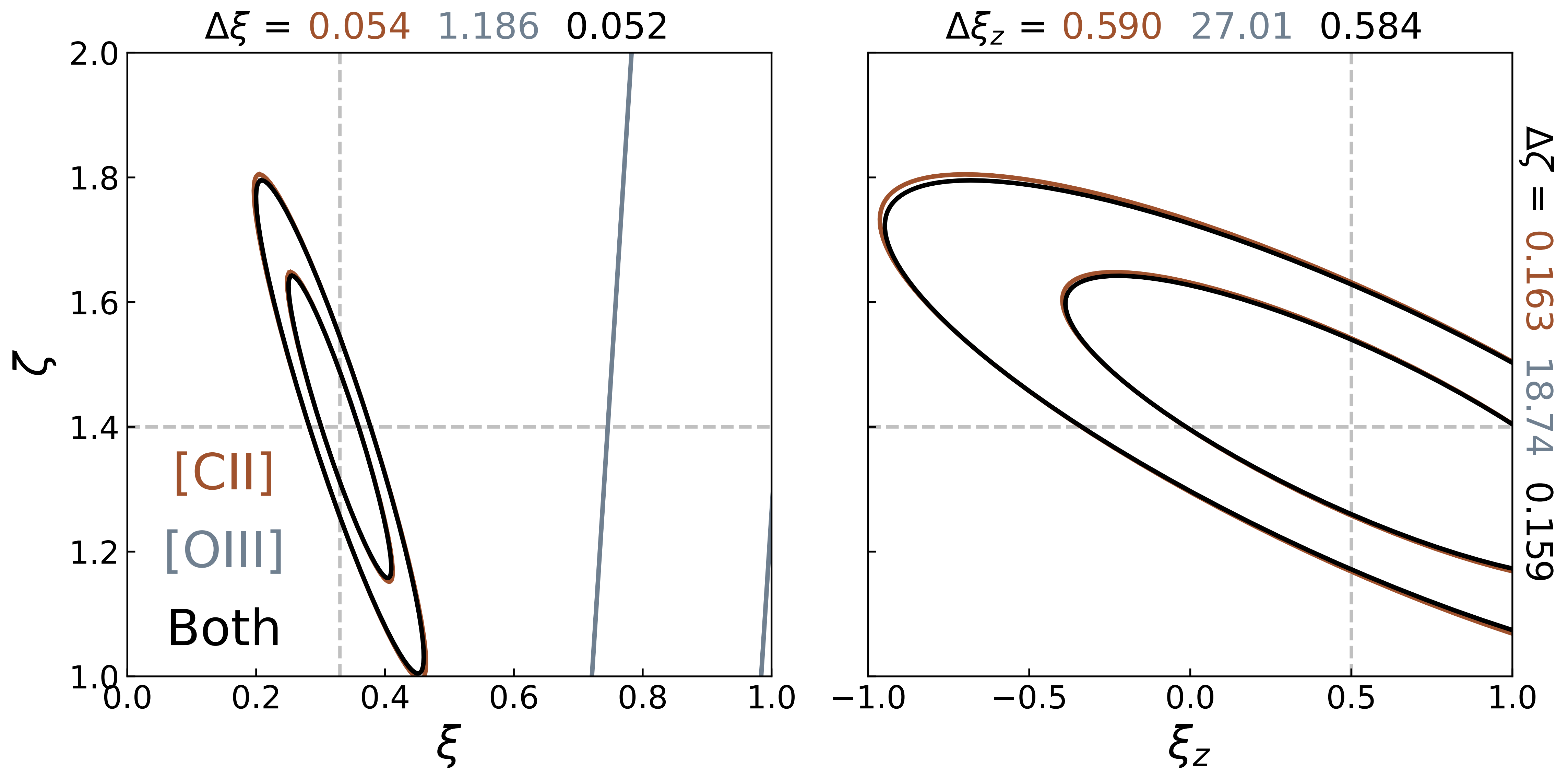

Future, space-based

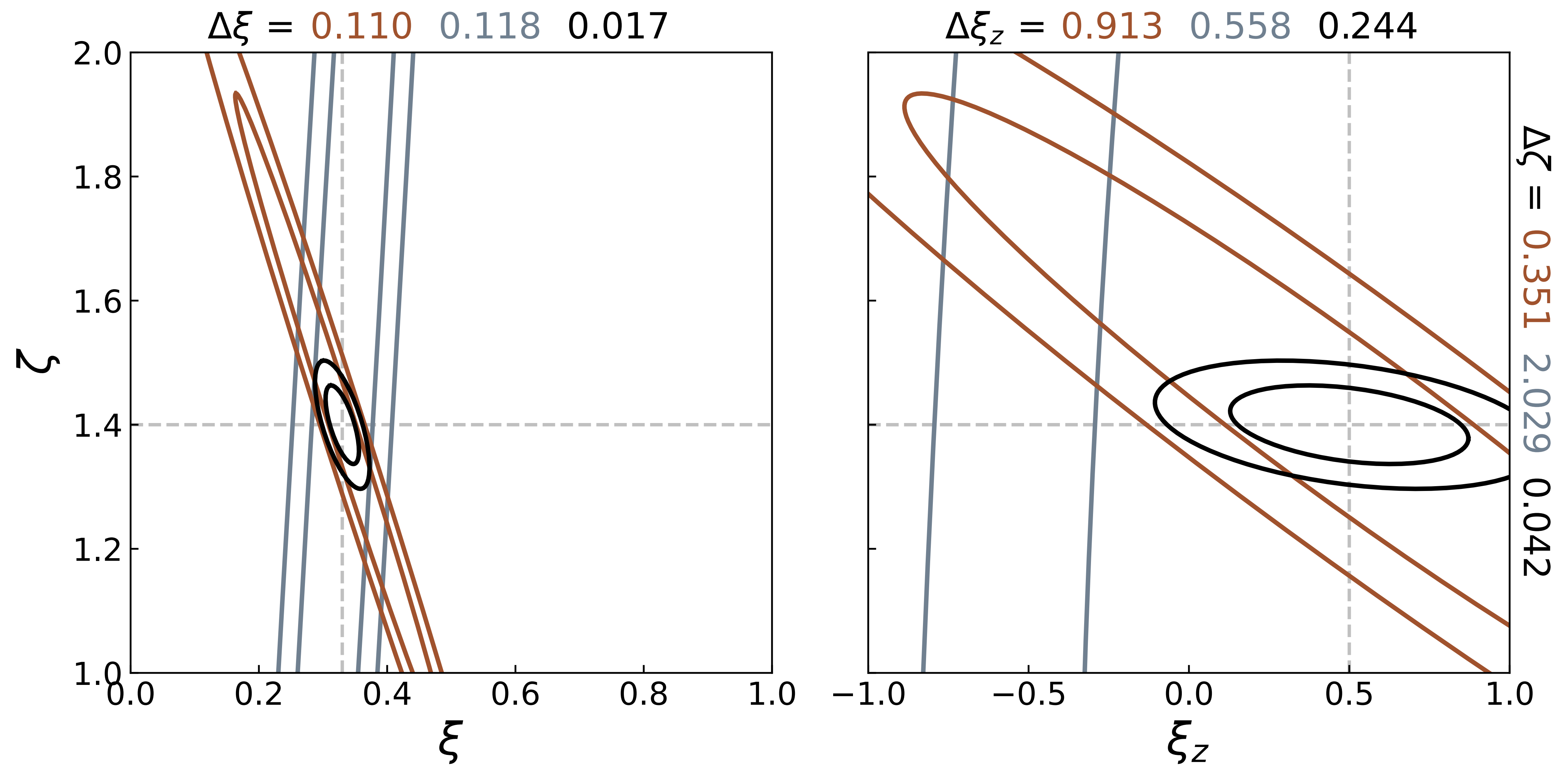

Implicit likelihood inference (ILI) w/ LIMFAST-simulated PS

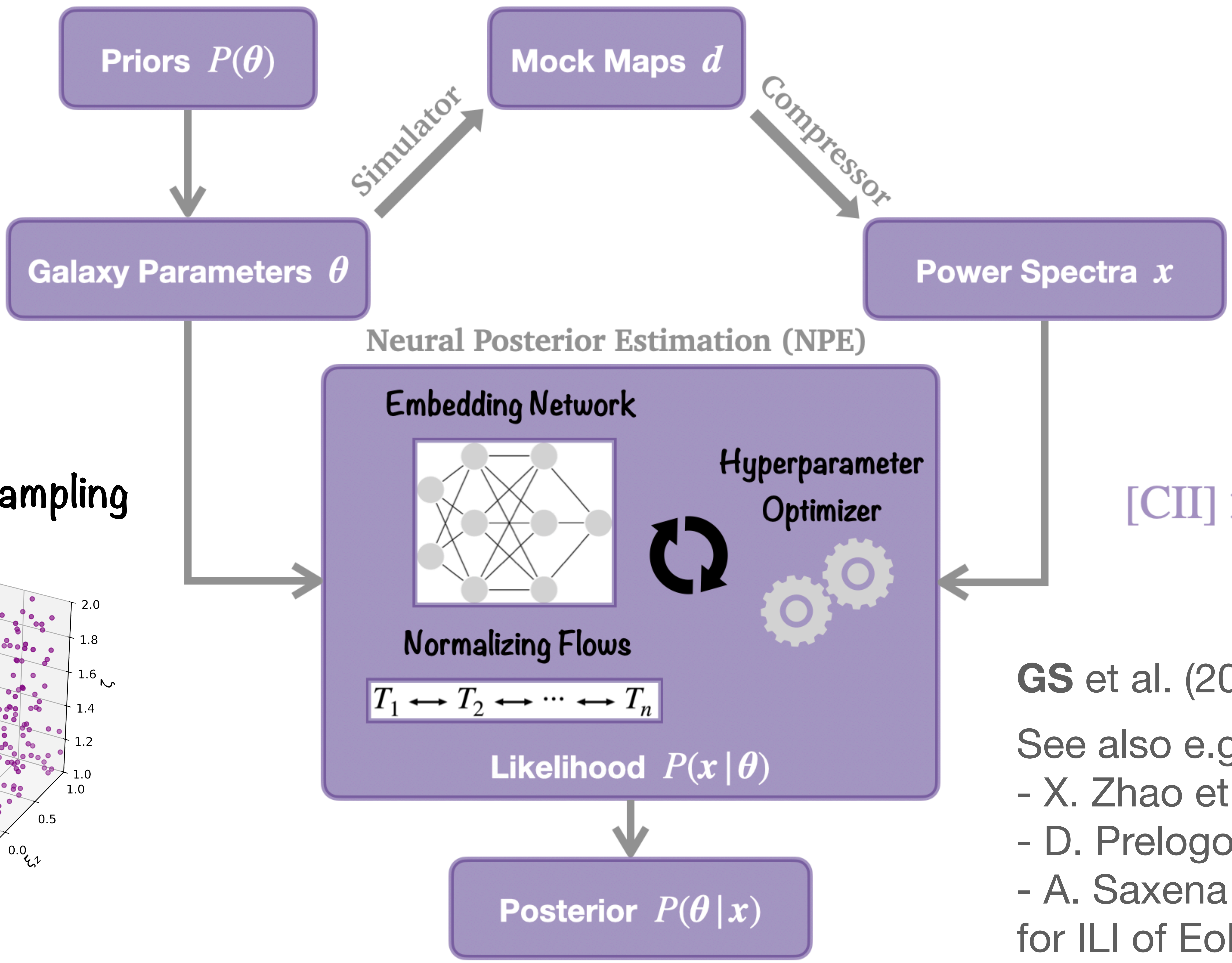

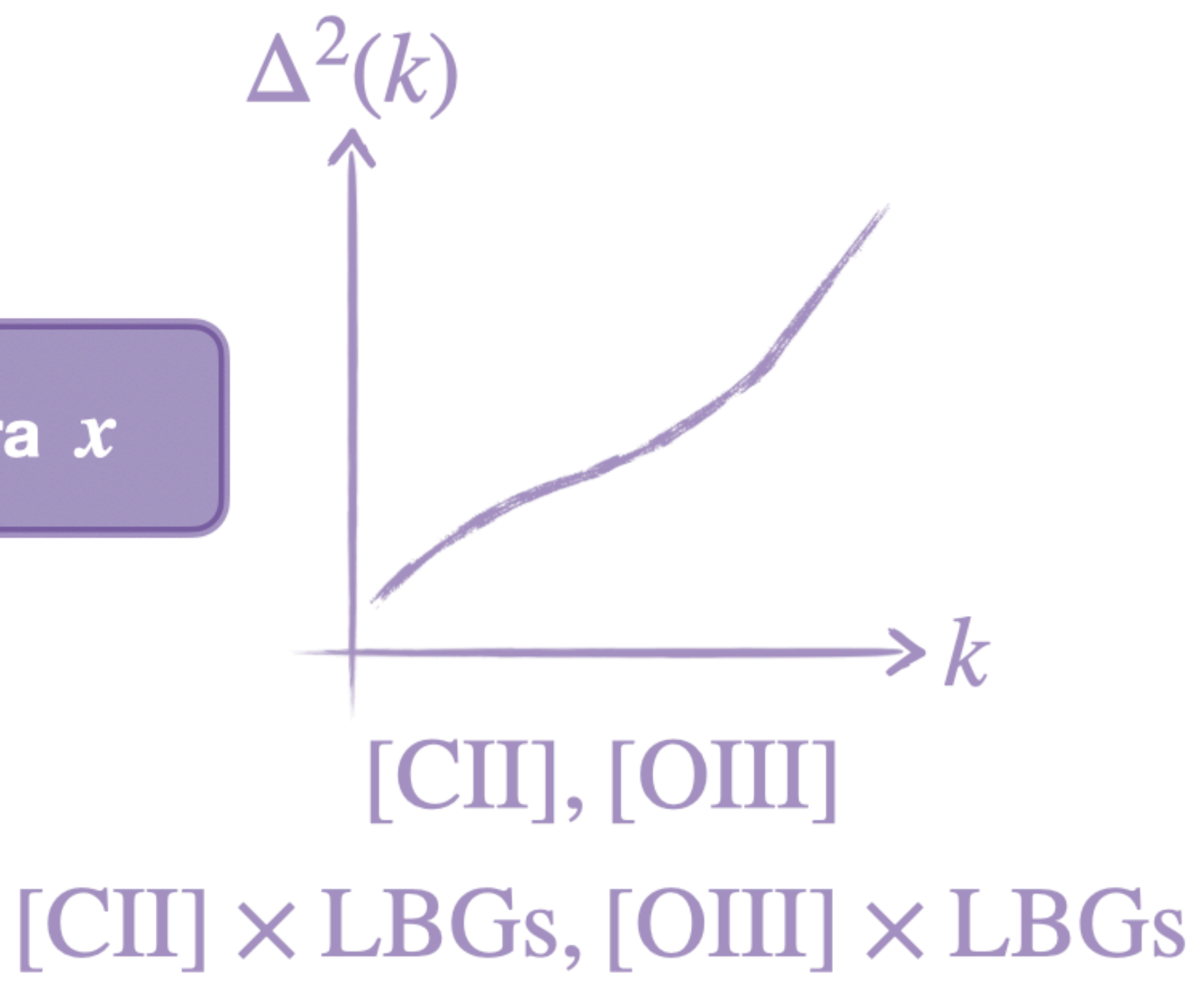

Latin Hypercube Sampling

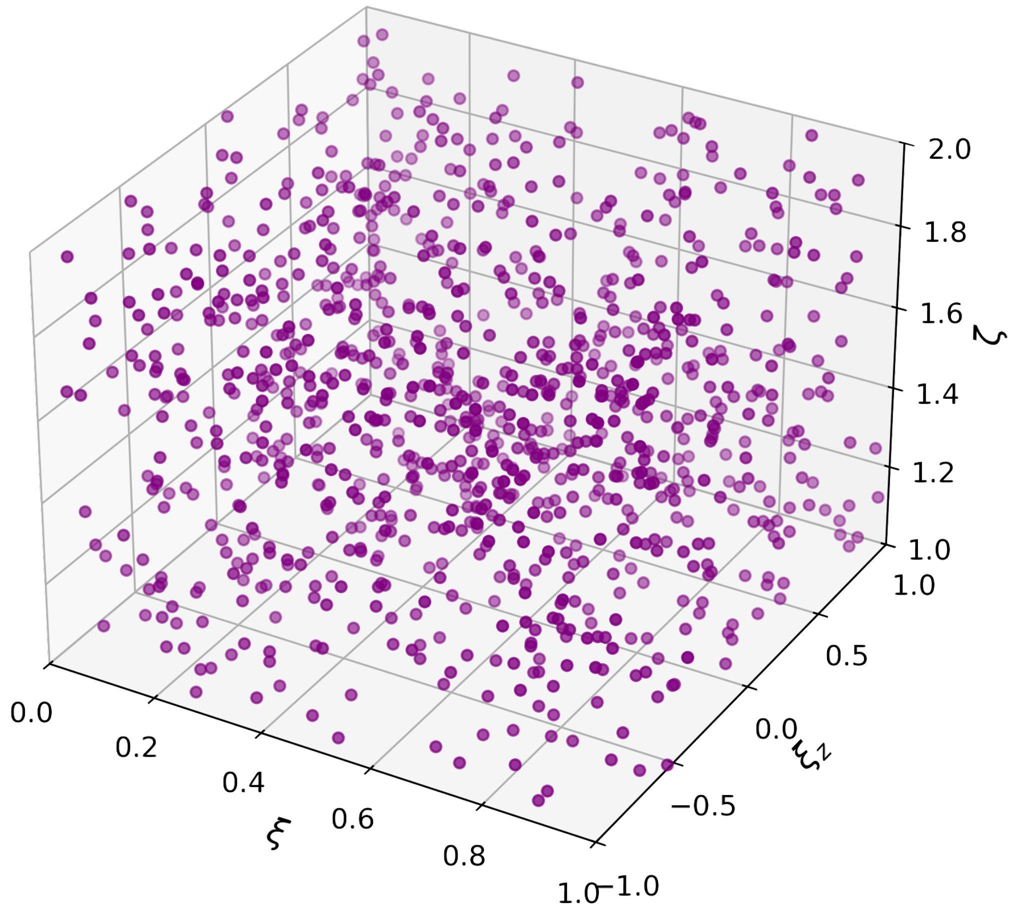

GS et al. (2025, in prep.)

See also e.g.,
- X. Zhao et al. (2022),
- D. Prelogović & A. Mesinger (2023)
- A. Saxena et al. (2023)

for ILI of EoR parameters from 21cm PS

Posterior from ILI w/ vs. w/o combining [CII] and [OIII]

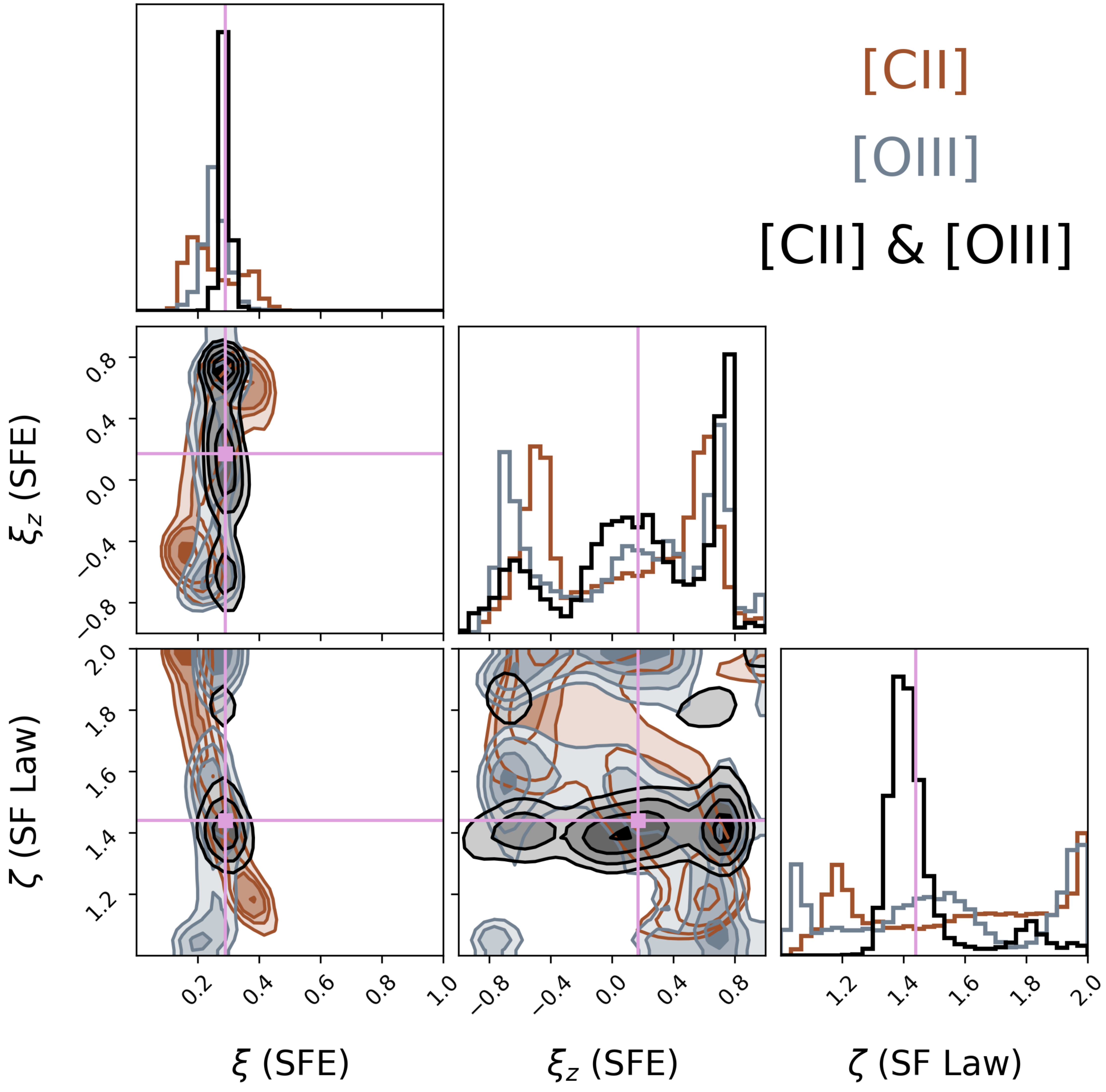

GS et al. (2025, in prep.)

- **ξ, ζ less degenerate w/ [CII] & [OIII]**
- **Constraint on ζ greatly tightened**

Validating posterior predictiveness & coverage from ILI

GS et al. (2025, in prep.)

Summary

- Multi-tracer IM provides a powerful way to statistically and collectively study physical processes that govern the formation and evolution of early galaxies.
- As mm wavelengths, combining [CII] and [OIII] LIM statistics (in foreseeable future) allows us to understand the SFE and SF law of high-redshift galaxies.
- Compared with traditional, explicit-likelihood methods, ILI enables more flexible and scalable analysis of galaxy formation physics using LIM summary statistics.

BACK UP SLIDES

Star formation efficiency (stellar mass-halo mass relation)

M. Shuntov et al. (2025)

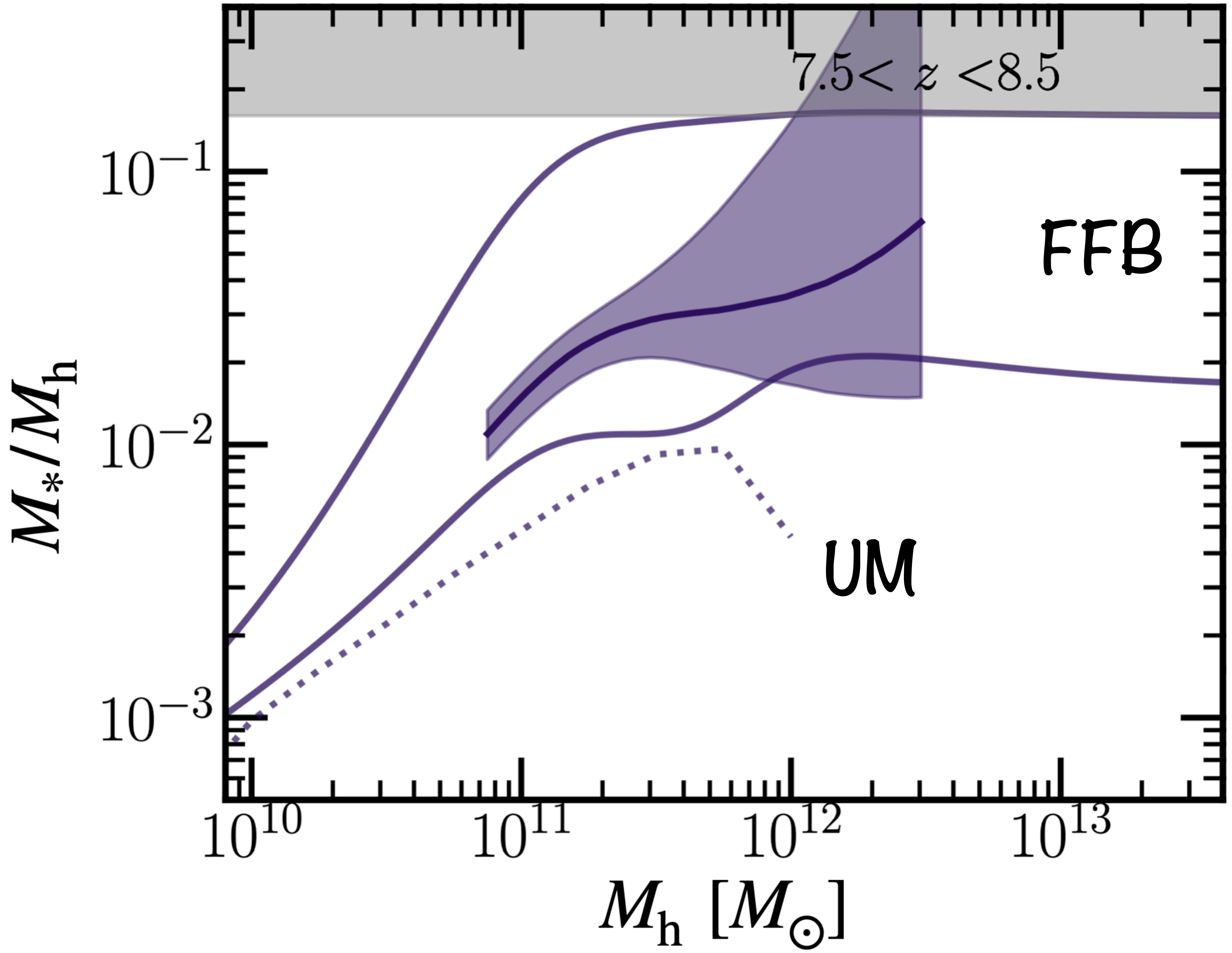

- **Probe of stellar feedback**
- **Mass & redshift dependence**

Star formation law (a.k.a. Kennicutt-Schmidt relation)

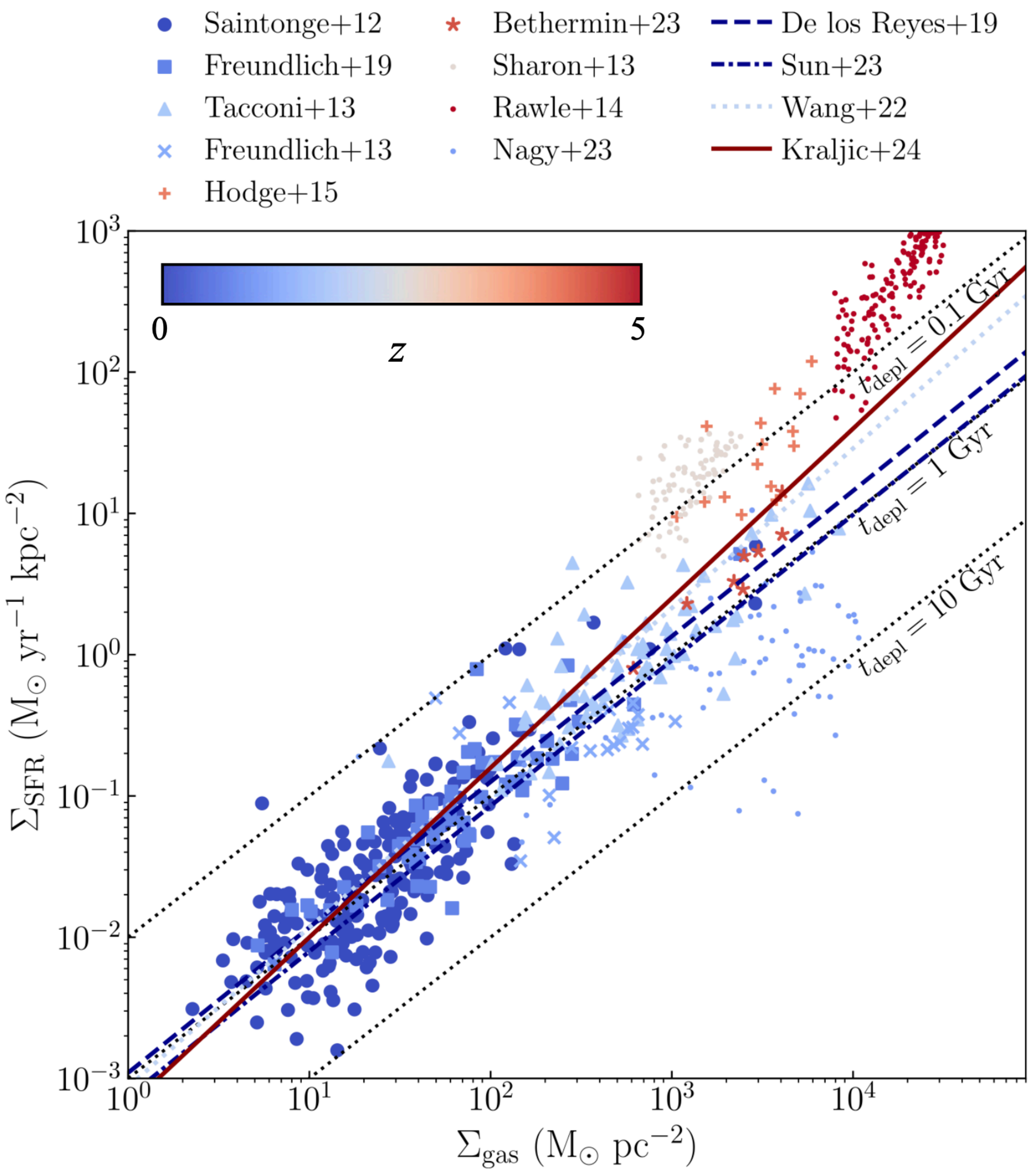

J. Freundlich et al. (2024)

- **Surface densities & gas depletion time**
- **Slope: denser gas better at SF (if > 1)**